

Chemical Characterization of Aerosols on the East Coast of the United States Using Aircraft and Ground-Based Stations during the CLAMS Experiment

ANDRÉA D. DE ALMEIDA CASTANHO,^{*} J. VANDERLEI MARTINS,^{+,#} PETER V. HOBBS,[@]
PAULO ARTAXO,^{*} LORRAINE REMER,[#] MARCIA YAMASOE,[&] AND PETER R. COLARCO^{**,#}

^{*}*Institute of Physics, University of São Paulo, São Paulo, Brazil*

⁺*JCET, University of Maryland, Baltimore County, Baltimore, Maryland*

[#]*NASA Goddard Space Flight Center, Greenbelt, Maryland*

[@]*Department of Atmospheric Sciences, University of Washington, Seattle, Washington*

[&]*Institute of Astronomy, Geophysics and Atmospheric Sciences, University of São Paulo, São Paulo, Brazil*

^{**}*Earth System Science Interdisciplinary Center, University of Maryland, College Park, College Park, Maryland*

(Manuscript received 16 October 2003, in final form 28 June 2004)

ABSTRACT

The Chesapeake Lighthouse and Aircraft Measurements for Satellites (CLAMS) experiment was carried out off the central East Coast of the United States in July 2001. During CLAMS, aerosol particle mass was measured at two ground stations and on the University of Washington's Convair 580 research aircraft. Physical and chemical characteristics of the aerosols were identified and quantified. Three main aerosol regimes were identified in the region and are discussed in this work: local pollution/sea salt background, long-range transported dust, and long-range transported pollution. The major component measured in the fine mode of the aerosol on the ground at Wallops Island, Virginia, was sulfate, estimated as NH_4HSO_4 , which accounted for $55\% \pm 9\%$ on average of the fine particle mass (FPM) during the experiment period. Black carbon concentrations accounted for $3\% \pm 1\%$ of FPM; soil dust was also present, representing on average $6\% \pm 8\%$ of FPM. The difference between the sum of the masses of the measured compounds and the total fine particle mass was $36\% \pm 10\%$ of FPM, which is attributed primarily to nitrates and organic carbon that were not measured. Aerosol chemical composition in the atmospheric column is also discussed and compared with ground-based measurements. Aerosol dust concentration reached 40% of FPM during an incursion of Saharan dust between 24 and 26 July. Sulfate aerosol reached 70% of FPM during the transport of regional pollution on 17 July. Moderate Resolution Imaging Spectroradiometer (MODIS) aerosol optical thickness, coupled with air parcel back trajectories, supported the conclusion of episodes of long-range transport of dust from the Sahara Desert and pollutants from the continental United States.

1. Introduction

Aerosol particles are important constituents of the atmosphere. Many of them are efficient at scattering and absorbing solar radiation, thereby producing direct radiative forcing. Through clouds, aerosols particles can also produce indirect radiative forcing and change cloud microstructures and possibly precipitation. In the past few decades many techniques have been used to characterize aerosol particles in the atmosphere and their effects on climate and human health. The *Terra* satellite, launched in December 1999 (see <http://terra.nasa.gov/>), opened a new era for the remote sens-

ing of aerosols from space using aerosol-specific sensors and algorithms.

The Chesapeake Lighthouse and Aircraft Measurements for Satellites (CLAMS) field experiment, carried out from 30 June to 1 August 2001 on the East Coast of the United States, was designed to obtain airborne measurements of the atmospheric and surface properties in order to validate products derived from remote sensing instruments aboard *Terra* (Smith et al. 2001), and to serve as a laboratory for testing and developing new remote sensing and in situ measurement techniques. In this paper we use a combination of in situ, ground-based, and aircraft aerosol filter sampling, ground-based [Aerosol Robotic Network (AERONET)] and space-based [Moderate Resolution Imaging Spectroradiometer (MODIS; on board *Terra*)] remote sensing, and air mass trajectory models to characterize the aerosol particles present in the CLAMS experimental region during the period of the experiment.

Corresponding author address: Andréa D. de Almeida Castanho, Institute of Physics, University of São Paulo, Rua do Matão, Travessa R, 187-Cidade Universitária, 05508-900 São Paulo, SP, Brazil.
E-mail: castanho@if.usp.br

2. Methods

During the period of the CLAMS field experiment two ground-based stations and one aircraft were used to characterize the chemical composition, mass concentration, optical equivalent black carbon (BC) content, and the absorption properties of aerosol particles at the surface and in the lower troposphere. One of the sampling stations was located at the main target of the experiment at the Chesapeake Lighthouse [hereafter called COVE [Clouds and the Earth's Radiant Energy System (CERES) Ocean Validation Experiment]]. The Chesapeake Lighthouse is an ocean platform located 25 km from Virginia Beach, Virginia (36.9°N, 75.7°W). The other ground station was on the top of a building in an isolated area (away from local sources of pollutants) of the National Aeronautics and Space Administration (NASA) Wallops Flight Facilities, Virginia (120 km from the lighthouse), at 37.8°N, 75.5°W.

The instruments at COVE operated with an integration time of 12 h from 0730 to 1930 (day) and from 1930 to 0730 (night) local time from 14 to 31 July. During this period, aerosol particle mass was sampled each day on a number of 23 Nuclepore filters and 23 Teflon filters at the lighthouse. The sampling systems were located at the top of the lighthouse tower, 35 m above sea level. The instruments at the Wallops aerosol sampling site also operated with an integration time of 12 h at the same local time from 30 June to 1 August. The sampling system was located on the flat roof of a building at about 15 m above the ground. On each day aerosol particle mass was sampled on a number of 66 Nuclepore filters and 58 Teflon filters at the Wallops site.

At the two ground-based stations, aerosol particles were sampled using stacked filter units (SFUs; Hopke et al. 1997) on 25-mm-diameter Nuclepore polycarbonate filters, in two separated size fractions. The inlet has an impactor stage designed to have 50% collection efficiency at 10- μm -equivalent aerodynamic diameter. Coarse particles ($2.5 < d_p < 10 \mu\text{m}$) were collected in an 8.0- μm pore-size filter, and fine particles ($d_p < 2.5 \mu\text{m}$) were collected on 0.4- μm pore-size filters. At a flow rate of 16 L min^{-1} , the unit acted as a dichotomous sampler (Hopke et al. 1997). On the aircraft, aerosol particles were sampled only in fine fraction filters since the aircraft inlet did not allow the sampling of particles with diameters larger than about 3 μm .

Mass concentrations of the fine and coarse modes were measured gravimetrically using a 1- μg sensitivity electronic microbalance in a controlled chamber (20°C, 50% relative humidity, with fluctuations less than 10% of these set points). The filters were equilibrated in the chamber for 24 h before being weighed. Electrostatic charges were controlled using radioactive sources. The concentration of optical BC on the fine fraction of the SFU was determined using a reflectance technique [compared with other methods by Reid et al. (1998)] that was calibrated using Monarch 71 soot carbon stan-

dard. Black carbon concentrations correspond to optically equivalent BC, assuming a BC absorption efficiency of 6.8 $\text{m}^2 \text{g}^{-1}$. Based on the measurement precision of the instrumentation, fine particulate mass (FPM) and black carbon concentration uncertainties are around 10 to 50 ng m^{-3} .

The elemental composition of the particles was determined by particle-induced X-ray emission (PIXE; Campbell 1995) at the 1.7-MV tandem Pelletron accelerator at the Laboratory of Analysis of Materials by Ionic Beam (LAMFI) at São Paulo University (Artaxo and Orsini 1987; Tabacniks et al. 1987). It was possible to measure the elemental concentration of up to 20 elements (Al, Si, P, S, Cl, K, Ca, Ti, V, Cr, Mn, Fe, Ni, Cu, Zn, Br, Rb, Sn, Zr, and Pb). The typical precision of the elemental concentration is 4% to 8%.

Aerosol samples were also collected at various locations off the central East Coast of the United States aboard the University of Washington's Convair 580 (CV-580) research aircraft during a total of 45 h in 10 flights in July 2001 (Magi et al. 2005). In each flight, the aircraft generally flew between 0.17 and 3.3 km above sea level. A total of 23 aerosol samples was collected on Nuclepore filters using the bag-house system described by Magi and Hobbs (2003). Some aerosol samples were also collected in a straight continuous flow line. Aerosol elemental composition, mass concentration, BC content, and absorption properties of the particles were measured as a function of the aircraft altitude and location.

Spectral aerosol optical thickness and particle volume size distribution were derived from sun photometer measurements located at Wallops and at COVE. The sun photometers were automatic sun-/sky-scanning radiometers and part of AERONET, which is distributed throughout the world (Holben et al. 1998).

Principal factor analyses (PFA) were used to identify the sources of pollutants (Thurston and Spengler 1985). The PFA model is based on the eigenvalue and eigenvector analysis of the correlation matrix of the normalized elemental concentration. The aim is to obtain a reduced number of factors (representing the sources) that are independent, uncorrelated, and explain most of the original data variability. The factor-loading matrix represents the association between the trace elements and each factor obtained. The factor scores are an indication of the strength of each sample to each retained factor. The percentage of variance explained for each variable can be used to test the effectiveness of the factor model to that particular variable. Also, the total variance explained by the model can be used as a check if the number of factors and their composition is adequate to the original database (Hopke 1991).

Airmass back trajectories were analyzed with the NASA Goddard Space Flight Center trajectory model (Schoeberl and Sparling 1995) for several initial times during the CLAMS experiment. At each starting time we ran 100 parcels uniformly spaced within a $1^\circ \times 1^\circ$

box centered over the CLAMS site at each of four initial altitudes (500, 1000, 2000, and 3000 m). The trajectories were run kinematically using the National Centers for Environmental Prediction (NCEP) Global Forecast System assimilated meteorology (Kalnay et al. 1990) with horizontal resolution of $1^\circ \times 1^\circ$. Vertical winds were computed from the divergence of the input horizontal winds. Trajectories were computed with a fourth-order Runge–Kutta scheme using a time step of 1/100 day.

The spatial distribution of aerosol optical thickness was derived from the MODIS sensor aboard the Earth Observing System (EOS) *Terra* satellite. *Terra* flies in a near-polar orbit, with a daylight equator crossing time of about 10:30 A.M. The aerosol optical thickness is derived operationally over land and ocean using different approaches, as described in detail by Kaufman et al. (1997) and Tanré et al. (1997). The aerosol optical thickness product shown in this work is a result of Gaussian-weighted averages of ± 5 days centered on the day of interest (giving highest weighting for the reported day) in order to cover for gaps due to sun glint and cloud contamination.

3. Results

a. Ground based

The PFA was performed with the elemental dataset of the fine and coarse particle mass for both ground stations. PIXE analysis results are available for 20 elements, but only those variables that were above the detection limit in all samples were included in the analysis (as shown in Tables 1 and 2). The PFA for both stations resulted in the same identified factors in fine and coarse modes. The last column in Tables 1 and 2 shows the values of the communalities, which are higher than 0.75 for all the variables, indicating the adequacy of the retained factors. The factors explained more than 95% of the total variance of the dataset. The factor-loading matrix for the fine fraction ($d_p < 2.5 \mu\text{m}$) of particle mass sampled at Wallops (47 samples) and COVE (14 samples) is shown in Table 1. The results for fine-mode aerosols showed a soil dust (Al, Si*, Ti, Fe*, Ca*, K*), an oil combustion (V*, Ni*), and a regional pollution source (S*, FPM*, BC*, Zn*, Pb*, Br, Se) for both stations (only the elements marked with an asterisk were above the detection limit on all samples from COVE). Although the sampling sites' locations are under strong influence of the marine emissions, Table 1 shows the strong association of S with BC and other pollutants with high communality value, indicating its origin in the regional air pollution.

The factor-loading matrix for the coarse fraction ($2.5 < d_p < 10 \mu\text{m}$) of the particle mass sampled at Wallops (46 samples) and COVE (14 samples) is presented in Table 2. Four main sources of coarse particle mass (CPM) were identified for both stations: soil dust (Si, Fe, Al, Ti, Ca, and also Sr and K), marine [Cl, Sr, K,

TABLE 1. Factor-loading matrix for the elemental FPM and BC concentrations of the fine-mode aerosol particles sampled at ground level at Wallops Island (_W) from 30 Jun to 1 Aug 2001 and at COVE lighthouse (_L) from 14 to 31 Jul 2001. Bold entries signify factor loadings greater than 0.4.

Element	Factor 1	Factor 2	Factor 3	Communalities
	Regional pollution	Soil dust	Oil combustion	
S_W	0.92		0.21	0.88
Pb_W	0.91			0.85
Se_W	0.91		0.22	0.88
FPM_W	0.91	0.13	0.26	0.92
Zn_W	0.86	0.20		0.80
BC_W	0.86	0.20	0.10	0.79
Br_W	0.85		0.12	0.75
Fe_W		0.98	0.16	0.99
Si_W		0.97	0.19	0.98
Ca_W	0.17	0.96		0.96
Ti_W	0.10	0.96	0.19	0.98
Al_W		0.95	0.22	0.96
K_W	0.39	0.86	0.14	0.92
V_W	0.19	0.33	0.91	0.98
Ni_W	0.29	0.29	0.89	0.96
Variance (%)	53	29	9	91
Zn_L	0.98	0.14		0.98
S_L	0.97		0.15	0.96
BC_L	0.96	0.19		0.96
FPM_L	0.94	0.21		0.94
Pb_L	0.85	0.18	0.31	0.84
Si_L		0.99		0.99
Fe_L	0.11	0.99		0.99
Ca_L	0.14	0.98		0.99
K_L	0.23	0.96		0.98
Ni_L	0.20		0.97	0.98
V_L		0.18	0.97	0.97
Variance (%)	53	27	16	96

with contributions of Ca and CPM (for Wallops) and S in both stations], regional pollution (Zn), and a fourth factor (S) called a sulfate source. The elemental concentration of coarse S has a significant association with the marine source in both stations. This represents the contribution of the natural marine-derived sulfate. The coarse sulfate in the COVE site is also associated with the soil dust source. This association might be due to the absorption of sulfur dioxide by the soil dust particles coming from the continent (which have an atmosphere enriched by SO_2).

A correlation analysis between the sources identified by PFA for fine and coarse modes of the aerosol and both stations is presented in Table 3. Only the statistically significant ($\geq 99\%$ confidence level) correlation coefficients (R) are shown. The soil dust components identified in the fine and coarse modes for each ground-based station were highly correlated with each other ($R = 0.9$; see Table 3). The same correlation was also observed for the regional pollution component, as shown in Table 3 for Wallops Island and for COVE. The high correlation between the fine and coarse modes indicates that both fractions come from the same

TABLE 2. Factor-loading matrix for the elemental CPM concentrations of the coarse-mode aerosol particles sampled at ground level at Wallops Island (_W) from 30 Jun to 1 Aug 2001 and at COVE lighthouse (_L) from 14 to 31 Jul 2001. Bold entries signify factor loadings greater than 0.4.

Element	Factor 1	Factor 2	Factor 3	Factor 4	Communalities
	Soil dust	Marine	Regional pollution	Sulfate	
Fe_W	0.97	0.15	0.15		1.00
Si_W	0.97	0.16	0.14		0.99
Ti_W	0.96	0.16	0.16		0.99
Al_W	0.96	0.16	0.13	0.13	0.99
Ca_W	0.70	0.60	0.21		0.93
Cl_W		0.96			0.97
CPM_W	0.25	0.89		0.29	0.94
Sr_W	0.46	0.79	0.16	0.19	0.90
K_W	0.55	0.79		0.21	0.97
Zn_W	0.27		0.96		1.00
S_W	0.17	0.56		0.79	0.97
Variance (%)	45	34	10	8	97
Fe_L	0.95	0.22	0.18	0.12	0.99
Al_L	0.93	0.29	0.12	0.16	0.99
Si_L	0.93	0.22	0.22	0.19	0.99
Ca_L	0.92	0.24	0.30		0.99
Ti_L	0.91	0.18	0.30	0.22	1.00
K_L	0.85	0.47		0.21	0.99
CPM_L	0.82	0.33		0.27	0.91
Cl_L	0.22	0.90		0.13	1.00
Sr_L	0.63	0.76		0.13	0.99
Zn_L	0.26		0.92	0.11	0.97
S_L	0.40	0.56	0.29	0.66	0.99
Variance (%)	58	21	13	6.5	98

source (or at least are transported together). For Wallops, the coarse sulfate is well correlated with oil combustion ($R = 0.5$). This indicates another sulfate source in addition to the marine-derived sulfate already identified for the coarse mode.

A high correlation ($R = 0.9$) was also observed between COVE and Wallops for both the fine particle mass of soil dust and the regional pollution component (Table 3). The high correlation between the two sites indicates that these sources are not local. Therefore both stations are influenced by regional or long-range transport of soil dust and regional pollution. The correlation between oil combustion products between the two sites was below the confidence level of 0.99, indicating local pollution. Fishing boats, which are a source of oil prod-

ucts, were common around the COVE site. The coarse fractions did not present a correlation between the stations, indicating the predominance of local sources.

The concentrations of inorganic compounds in the FPM (for ground and aircraft samples) and CPM (for ground samples) were estimated based on elemental concentrations derived from PIXE. The sampling sites are under the influence of marine emissions. The marine contribution of sulfur is found in this analysis to be most important in the coarse mode of the aerosol. For the fine mode, most of the sulfur is considered to be from anthropogenically derived aerosol. The predominant form of fine sulfate in polluted air is the acid sulfate (NH_4HSO_4), as established by Weiss et al. (1982) and discussed by Hegg et al. (1997). Therefore, the sul-

TABLE 3. Correlation coefficients (R) between fine- and coarse-mode sources for Wallops and COVE ground-based stations. Also, correlation coefficients between Wallops and COVE for fine and coarse modes. Only the statistically significant ($\geq 99\%$ confidence level) correlation coefficients are shown.

		Wallops				COVE		
		Soil dust	Marine	Regional pollution	Sulfate	Regional pollution	Soil dust	Oil combustion
		Coarse				Fine		
Wallops	Regional pollution	Fine	—	—	0.48	—	0.95	—
	Soil dust		0.88	—	—	—	0.88	—
	Oil comb		—	—	—	0.50	—	—
COVE	Soil dust	Coarse	—	—	—	—	0.95	—
	Marine		—	—	—	—	—	—
	Regional pollution		—	—	—	—	0.86	—
	Sulfate		—	—	—	—	—	—

fate compound was estimated by multiplying the sulfur concentrations by a factor of 3.59. Another sulfate form in a regional pollution area with sufficient ammonia is ammonium sulfate $[(\text{NH}_4)_2\text{SO}_4]$ (Sweet and Gatz 1998). If ammonium sulfate were the predominant form of sulfate, a correction factor of 1.15 would have to be applied to the results presented here for the acid sulfate compound. For the coarse mode, the PFA indicates the S associated with three different sources. Since the partitioning of sulfur among each source is not precisely known, the S coarse mass was added to the nonmeasured compounds, called “other compounds.” Another compound identified by the factor analyses was soil dust. The soil dust fine and coarse mass was estimated by the sum of the oxides: aluminum $\times 1.89$, silicon $\times 2.14$, titanium $\times 1.334$, calcium $\times 2.50$, potassium $\times 1.20$, and iron $\times 1.43$. The marine contribution to the coarse mode was estimated by considering the NaCl compound to be dominant, although we realize this neglects contributions from other sea salt compounds.

The optically equivalent BC concentration for the fine-mode particles was obtained using the broadband

reflectance technique. Organic carbon and nitrates were not measured in these samples. However, the non-measured compounds would be the difference between the measured compounds and the measured total fine mass concentration and are defined as the “other compounds” in the analysis.

The factor defined as other compounds, in the fine mode, is composed of organic carbon, nitrates, and all unmeasured mass. This factor presented high correlation ($R = 0.84$ and 0.9) at both stations to the fine regional pollution source (identified in PFA), indicating its regional pollution origin. The factor defined as other compounds of the coarse mode is composed of organic carbon, sulfates, nitrates, and all unmeasured mass. For the Wallops Island station this factor was highly correlated with the coarse marine source ($R = 0.7$), but was less correlated with the sulfate source ($R = 0.4$), indicating it is mainly of local marine source origin.

The average FPM and CPM at Wallops Island during the experimental period were $10 \pm 6 \mu\text{g m}^{-3}$ and $13 \pm 8 \mu\text{g m}^{-3}$, respectively. Time series of the FPM and the

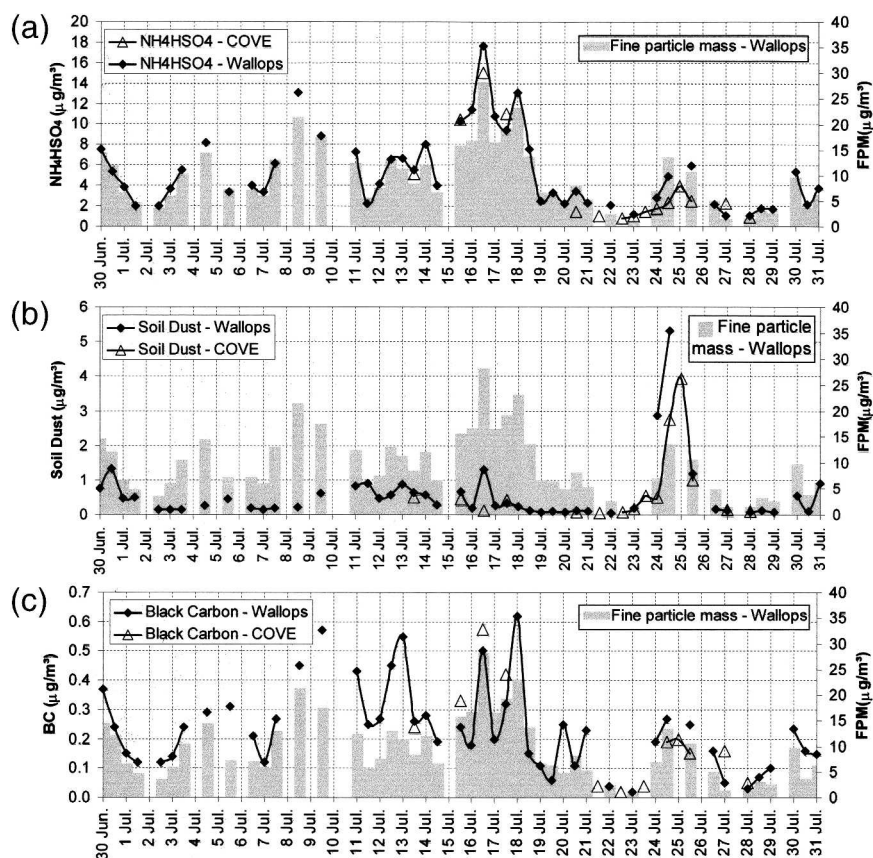


FIG. 1. Time series of mass concentration of FPM measured on the ground at Wallops Island, VA (FPM_W), compared to FPM in the form of (a) acid sulfate (NH_4HSO_4), (b) soil dust, and (c) BC, all measured on the ground at Wallops Island and at the COVE lighthouse (uncertainties are from 10 to 50 ng m^{-3}).

fine-mode concentration of the main compounds measured during the experiment are shown in Fig. 1. The sulfate and BC concentration have basically the same variability as the FPM concentration, which is consistent with the PFA results that indicate that they originate from the same source. The soil component shows a different variability, presenting an increase between 24 and 26 July, presumably because of its long-range transport (see section 3c). The time series for the coarse particle mass, NaCl, soil dust, and other compounds are presented in Fig. 2. The correlation of each component with the CPM can help identify the dominant sources of these components during various episodes of the experiment. The high correlation between NaCl and CPM shows the large contribution of sea salt to the coarse particle mode. The soil component shows a different variability as in the fine mode, presenting an increase between 24 and 26 July, presumably also because of its long-range transport (see section 3c).

The apportionment of the compounds in the FPM and CPM at Wallops Island were also estimated. There is a high correlation between most of the sources ob-

served at Wallops and for the COVE results. However, because of the different sampling period and number of samples, the COVE results are not shown here. The average fine acid sulfate concentration was $5 \pm 4 \mu\text{g m}^{-3}$, corresponding to $55\% \pm 9\%$ of the FPM. The average fine soil dust concentration was $0.6 \pm 0.9 \mu\text{g m}^{-3}$ corresponding to $6\% \pm 8\%$ of the total FPM. The higher variability of the soil dust component is due to periods of elevated concentrations of soil dust in the region, which are discussed below. The average BC concentration was $0.2 \pm 0.1 \mu\text{g m}^{-3}$ for FPM, which corresponds to $3\% \pm 1\%$ of the total FPM. For comparison, for the urban area of São Paulo, Brazil, the concentration of BC is on average 20% of the total FPM, and it can reach hourly means of $30 \mu\text{g m}^{-3}$ during episodes of high pollution; sulfate concentrations in São Paulo are about the same as those measured in CLAMS (Castanho and Artaxo 2001). Since we are comparing here optical equivalent BC, the difference between BC in CLAMS and São Paulo could be due to either an actual difference in concentrations or a different absorption efficiency of BC. The compounds not

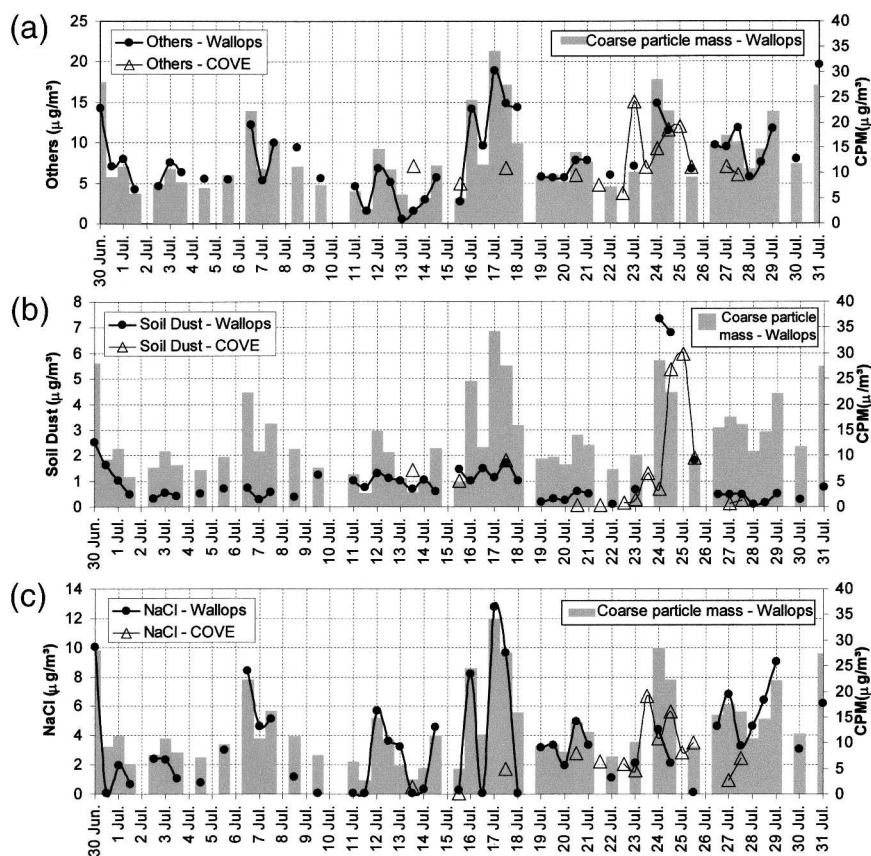


FIG. 2. Time series of mass concentration of CPM measured on the ground at Wallops Island compared to CPM in the form of (a) other compounds (compounds not measured plus S compounds not estimated), (b) soil dust, and (c) NaCl, all measured on the ground at Wallops Island and at COVE (uncertainties are from 10 to 50 ng m^{-3}).

measured in CLAMS account for 36% of the FPM. Since the fine other compounds are highly correlated to the regional pollution source, this makes it the major source of this fine particle mass. If organic carbon alone

were responsible for the 36% of the unaccounted FPM it would still be less than the column organic carbon obtained in previous measurements in the same general area by Novakov et al. (1997). According to Novakov et

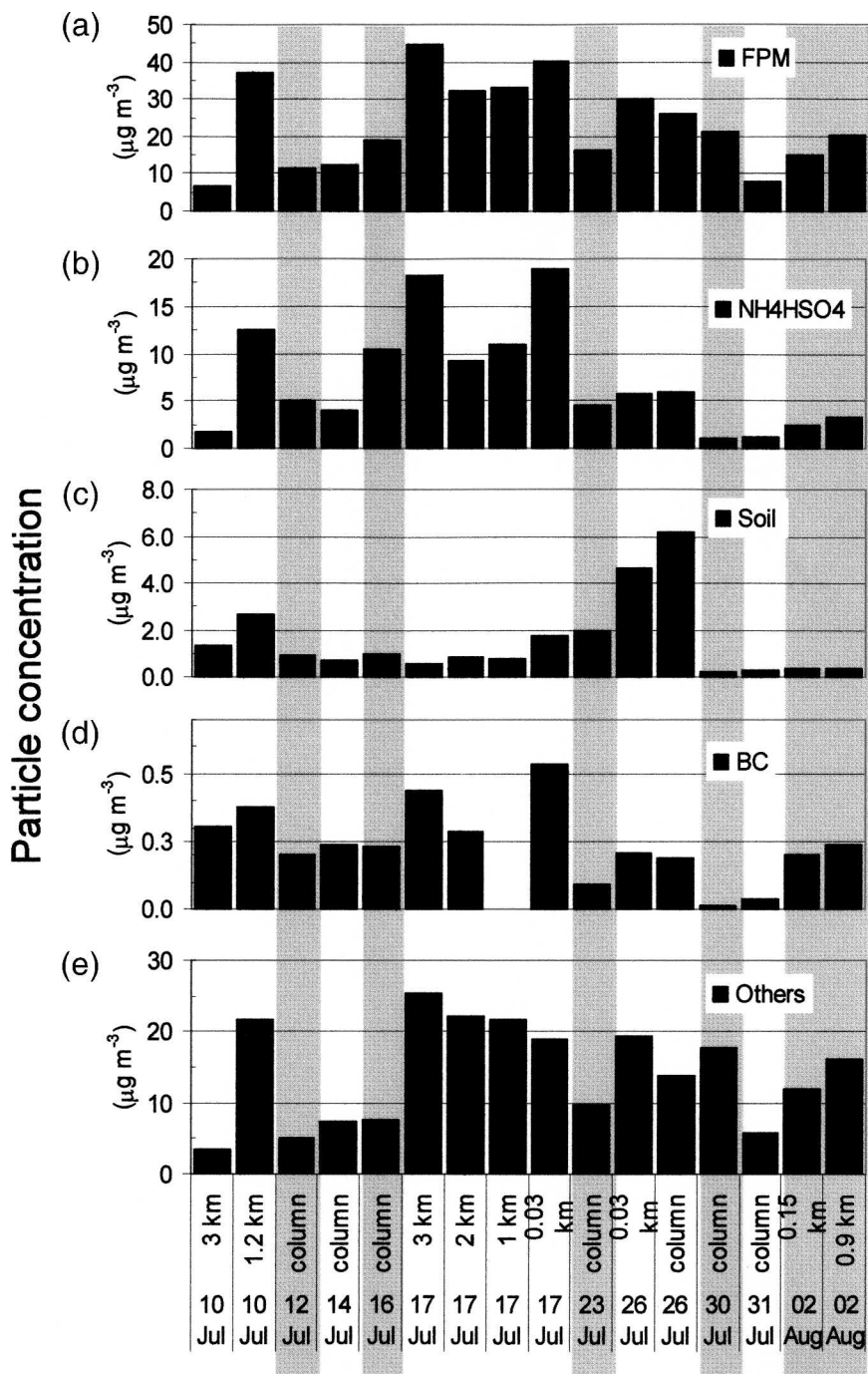


FIG. 3. Composition of aerosol FPM from filters exposed on the CV-580 aircraft in CLAMS: (a) total fine particle mass, (b) acid sulfate (NH_4HSO_4), (c) soil dust, (d) BC, and (e) difference between the total fine particle mass and the measured compounds (Others). The dates and altitudes of the samples are shown; "column" indicates integrated sample in vertical column. Note different scales on ordinates (uncertainties are from 10 to 50 ng m^{-3}).

al. (1997), the carbon mass fraction tends to increase with altitude, which agrees with our results showing lower carbon mass fraction in the ground-based measurements. The coarse-mode apportionment shows a soil dust concentration of $1.0 \pm 1.4 \mu\text{g m}^{-3}$ for CPM, corresponding to $9\% \pm 8\%$ of the total CPM. The average concentration of the NaCl compound in CLAMS was $3 \pm 3 \mu\text{g m}^{-3}$ for the coarse particle mode, which corresponds to $23\% \pm 15\%$ of total CPM. The compounds not measured in CLAMS account for 62% of the CPM. Since the other coarse compounds are highly correlated to marine source it is clear that the marine aerosol is the major source of the coarse particle mass on average in the studied sites.

b. Aircraft

Figure 3 shows the concentrations of compounds measured on various flights of the CV-580 in CLAMS. In some cases, because of low aerosol loadings, the samples collected in the airplane were integrated in the vertical column using multiple bag-house loads to ensure adequate filter loadings for accurate analyses. The mass concentration of the fine particulate in the vertical column averaged $23 \pm 12 \mu\text{g m}^{-3}$. Acid sulfate was, on average, $7 \pm 6 \mu\text{g m}^{-3}$, which is similar to that measured in the Tropospheric Aerosol Radiative Forcing Observational Experiment (TARFOX; $6 \pm 6 \mu\text{g m}^{-3}$). The acid sulfate fraction reached 40%–50% of the FPM

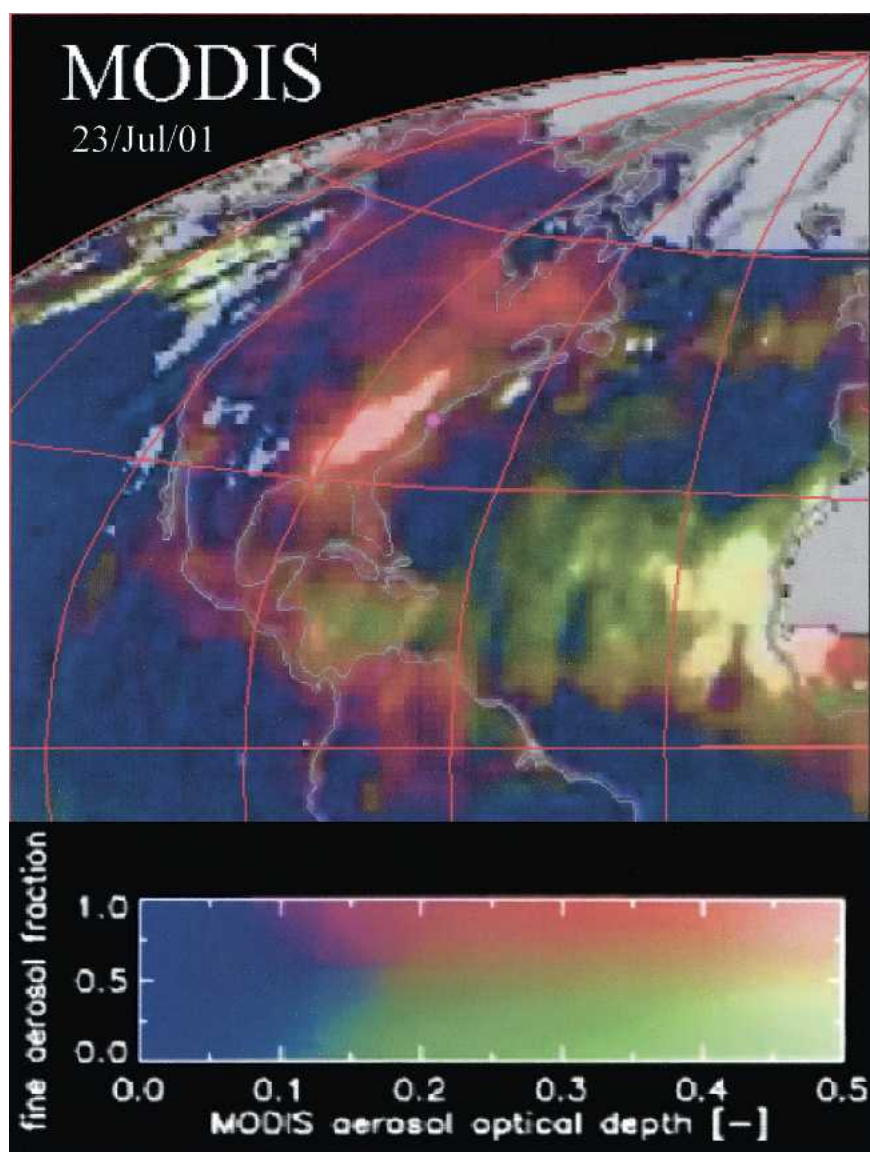


FIG. 4. Level 3 MODIS AOT fine and coarse aerosol fraction. A composition of Gaussian-weighted averages of ± 5 days centered on 23 Jul 2001 representing the overall pattern for the persistent distribution of the aerosol loading in the studied period.

during the most polluted days (e.g., 17 July) and dropped to 10%–20% on the less polluted days (30 July to 2 August). The opposite occurred with the fraction of the unmeasured compounds (organic carbon and nitrates), which were generally about 50% but increased to around 80% on the last few days of the study. On 17 July, adequate filter samples were obtained for quantitative analyses at four altitudes (Fig. 3). Elevated concentrations of FPM were measured at 3 km and near the surface, where high scattering coefficients were also measured (Magi et al. 2005). An enrichment of the regional pollution aerosol is shown on 17 July, as reflected in increases in the total FPM and NH_4HSO_4 . On 26 July the soil dust was unusually high, corresponding to the Saharan dust aerosols identified also in the

ground-based measurements discussed in detail in section 3c below.

c. Remote sensing and air parcel trajectory analyses

Figure 4 shows a composite of level 3 MODIS aerosol optical thickness (AOT) retrievals color coded to separate the fine- and coarse-mode aerosols (red = fine-mode aerosols, green = coarse-mode aerosols; here we use the retrieved fine-mode fraction to perform the separation). The MODIS daily data show gaps due to clouds, nonoverlap of orbits, and sun-glint reflection of the ocean. Despite these gaps, there is a persistent aerosol distribution in the region of interest, so it was decided to use the ± 5 days Gaussian-weighted MODIS averages, improving the visualization and facilitating

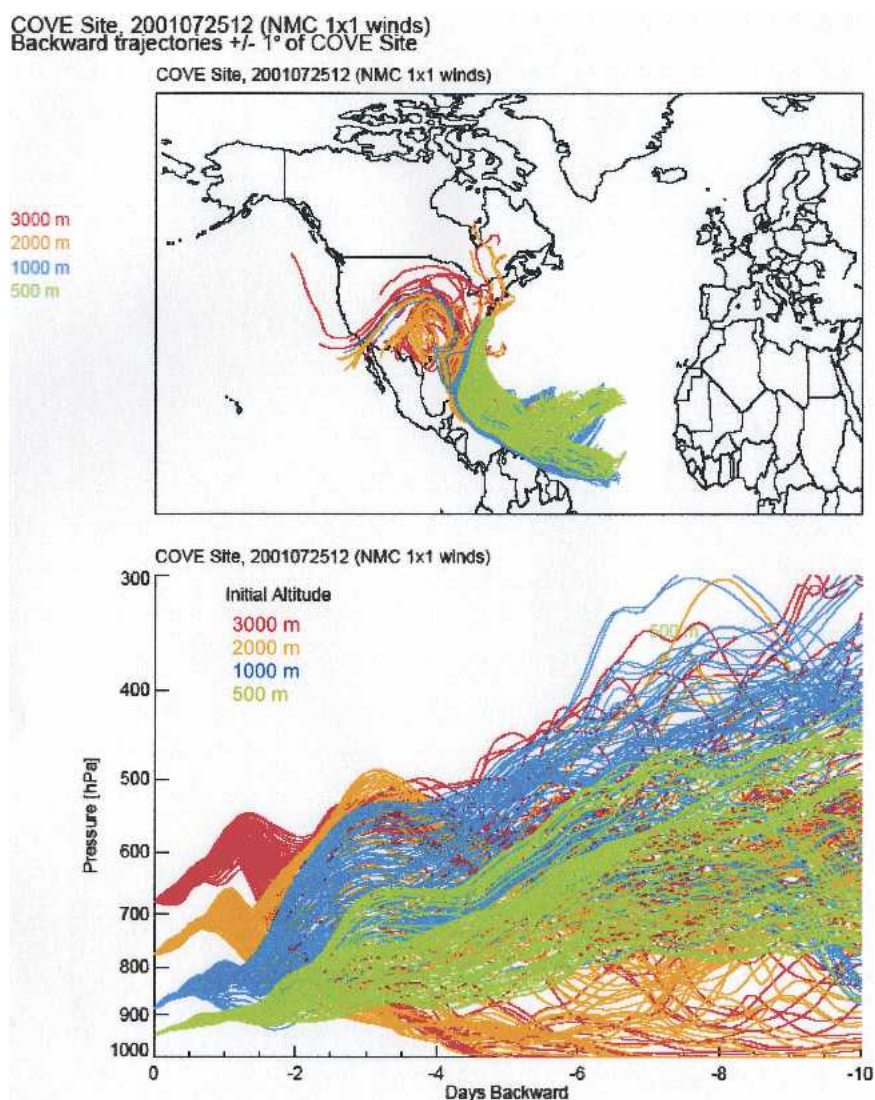


FIG. 5. Air mass back trajectories were run kinematically using the NCEP Global Forecast System assimilated meteorology. Starting time is 25 Jul at 1200:00 UTC of 100 parcels uniformly spaced within a $1^\circ \times 1^\circ$ box centered over the CLAMS site at each of four initial altitudes (500, 1000, 2000, and 3000 m represented as pressure).

the interpretation of the results. The MODIS image during the period shows the regional pollution of fine aerosols along the East Coast of the United States. There is also a high loading of aerosol across the North Atlantic Ocean, indicating the transport of soil dust from the Sahara Desert to the Caribbean Sea region. This overall pattern was observed during the whole period of the experiment and is represented by the image for 23 July shown in Fig. 4. The transport of the Saharan dust over the Caribbean region has been studied by many authors. Experimental evidence suggests the predominant transport mechanism is in the free troposphere, where the dust is rapidly transported across the Atlantic Ocean through the so-called Saharan air layer (SAL; Reid et al. 2003 ; Prospero et al. 1981). The Puerto Rico Dust Experiment (PRIDE) was carried out to better understand the issue of dust transport and

radiative forcing in the north subtropical Atlantic Ocean (Reid et al. 2003; Colarco et al. 2003; Levy et al. 2003). During PRIDE, the Saharan dust layer was observed most predominantly around 3 km, with events of vertical distribution from low levels up to 5-km altitude.

Both the ground-based stations and aircraft samples show an increase in the concentrations of soil dust reaching $5 \mu\text{g m}^{-3}$ (40% of FPM) compared to less than $1 \mu\text{g m}^{-3}$ (6% of FPM on average) shown in Figs. 1 and 3. The most intense soil dust episode started at the night of 24 July at Wallops Island and on 25 July during the day at COVE. At both sites the dust episode ended on 26–27 July. During the dust episode the Al/Ca ratios were around 3.5 at Wallops, which is consistent with the criteria for the identification of Saharan dust (Hegg et al. 1997). The coarse fraction of the soil dust also increased during this period, reaching $7 \mu\text{g m}^{-3}$ (30% of

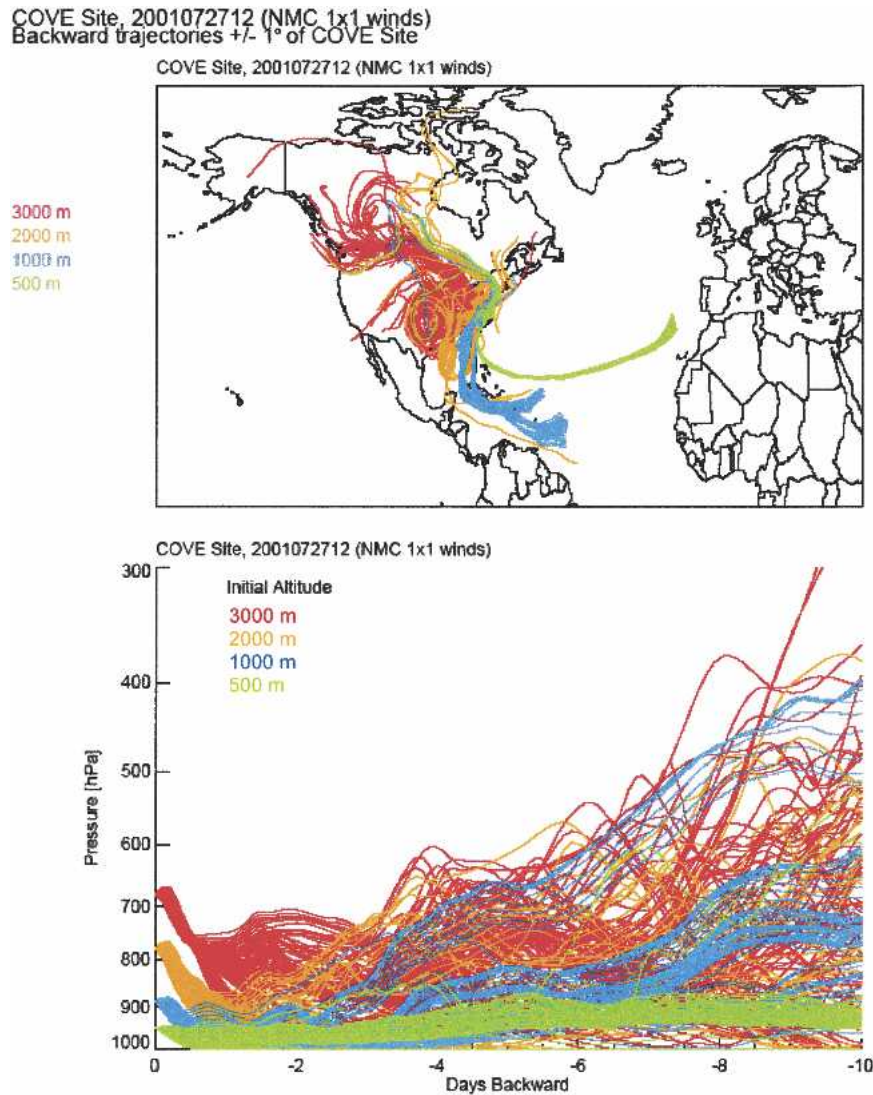


FIG. 6. As in Fig. 5, but for a starting time of 27 Jul at 1200:00 UTC.

CPM) shown in Fig. 2 compared to $1 \mu\text{g m}^{-3}$ (9% of CPM) on average.

Ten-day air parcel back trajectories were calculated for the CLAMS period. Figure 5 shows back trajectories beginning on 25 July. In 3 days backward trajectories show air parcels coming from the Caribbean Sea, where MODIS shows a large AOT because of Saharan dust particles (coarse particles). Despite the inherent uncertainties in trajectory models, the position of the air parcels for previous days (from 3 to 10 days backward) clearly shows air mass transport throughout the Atlantic Ocean. We ran trajectories for the whole period of the experiment. During July 2001, the trajectories showed their origins in the Caribbean Sea only on 1 July and during the period from 23 to 26 July. These results are very consistent with the period of soil dust episode shown in Figs. 1–3. The analyses of MODIS

and back trajectories confirm the transport of aerosol dust coming from the Sahara Desert and measured in the ground stations and aircraft.

The air parcels arriving at COVE on 27 July (Fig. 6) show changes in direction, suggesting the transport of dust-free air into the CLAMS region exactly when the chemical analyses results indicate the end of the soil dust episode. The following day, 28 July, shows all trajectories coming from the northeast for the first 3 days, confirming the end of the episode.

Figure 7 shows air parcel back trajectories for 17 July. The trajectories show air coming over the Great Lakes to the COVE site, presumably transporting pollutants (suggested by the red AOT in Fig. 4). The aerosol composition analyses from the ground stations (Wallops and COVE) and from the aircraft measurements on 17 July clearly show a regional pollution influence by the

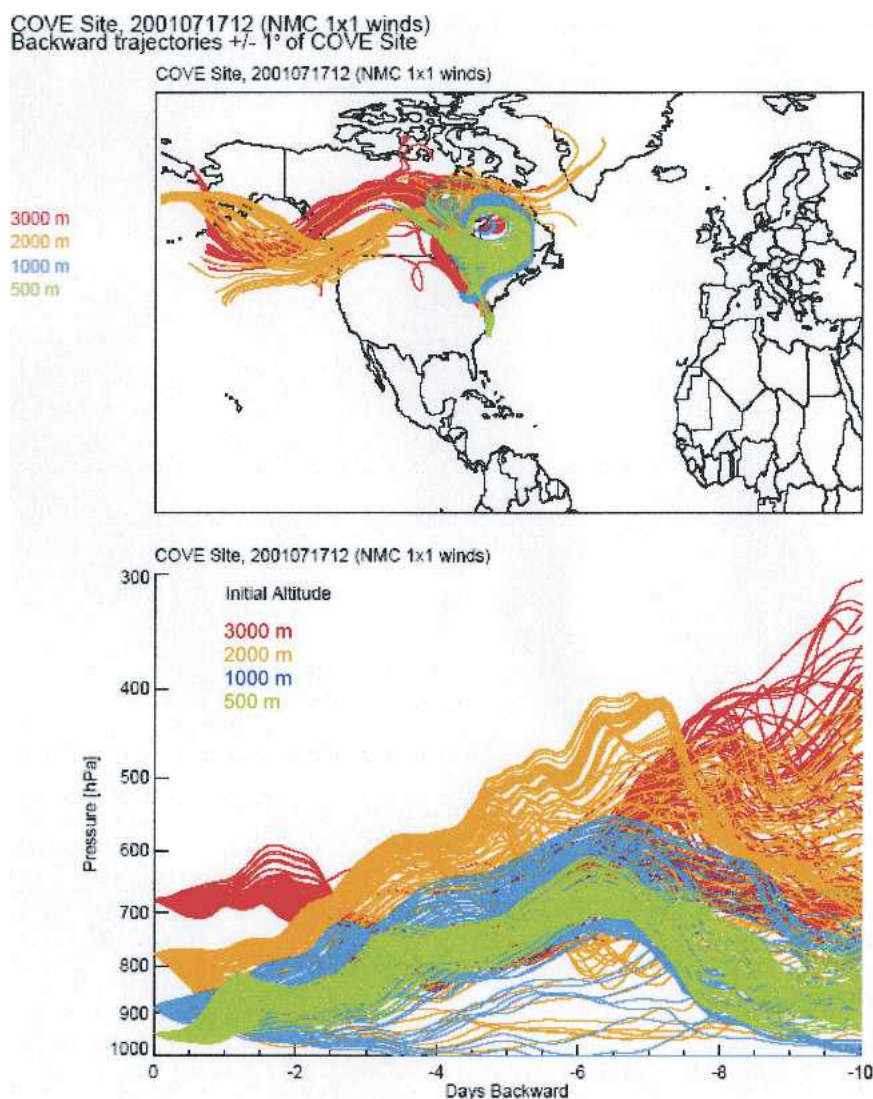


Fig. 7. As in Fig. 5, but for a starting time of 17 Jul at 1200:00 UTC.

increase in the sulfate concentrations up to $18 \mu\text{g m}^{-3}$ (70% of FPM) compared to $5 \mu\text{g m}^{-3}$ (55% of FPM on average for the period); there was no significant increase in the coarse mode because the acid sulfate is predominantly in the fine mode.

Changes in particle sizes were consistent with the chemical characterization of the episodes. Figure 8 shows size distributions in the three aerosol regimes as retrieved by AERONET. The first one is the regular background with pollution and sea salt predominantly in the fine mode, presented on 14 July. The particle size distribution showed a shift in the fine particle mode to larger particles on 24 July. This result is consistent with the increase in the soil mass (mainly characterized by larger particles) observed at the ground-based stations between 24 and 26 July. On 17 July the particle size distribution is predominantly in the fine mode, which is consistent with the sulfate composition discussed in the manuscript.

4. Conclusions

Three main aerosol regimes were identified during the period of the CLAMS field experiment: the local pollution/sea salt background, long-range transported dust, and regional U.S. East Coast pollution. The physical and chemical characteristics of these aerosol types have been quantified in this paper. The main sources of fine- and coarse-mode particles were soil dust (Al, Si, Ti, Fe, Ca, K), oil combustion (V, Ni), and regional pollution (S associated with fine particles, black carbon, Zn, and Pb). The ground-based and aircraft measurements showed a consistent pattern.

The average composition of the fine- and coarse-mode particles during the experiment was determined. For the fine mode, acid sulfate (NH_4HSO_4) was $55\% \pm 9\%$ of FPM, and black carbon was $3\% \pm 1\%$ of FPM. Soil dust was present at ground stations and represented, on average, $6\% \pm 8\%$ of the FPM and $9\% \pm 8\%$ of the CPM. Other compounds (not measured) ac-

counted for 36% of the FPM and 62% of the CPM; NaCl represented $23\% \pm 15\%$ of the CPM.

During the CLAMS experiment, two long-range transport episodes significantly influenced the aerosol composition. From 24–26 July, the long-range transport of soil dust increased the concentration of soil-dust-derived particles to $\sim 5 \mu\text{g m}^{-3}$ (40% of the FPM) compared to $< 1 \mu\text{g m}^{-3}$ (6% of the FPM) during the remainder of the experiment. On 17 July, there was an enhancement of regional pollution aerosols with an increase in sulfate concentration to $18 \mu\text{g m}^{-3}$ (70% of FPM), compared to an average concentration of $5 \mu\text{g m}^{-3}$ (55% of the FPM) during CLAMS. MODIS aerosol optical thickness measurements, coupled with air parcel back trajectories, showed that the soil particles that reached the central East Coast of the United States on 24–26 July derived from the Sahara Desert, and the regional pollution aerosol on 17 July was due to regional U.S. East Coast air pollutants.

Acknowledgments. We thank Dr. Ken Rutledge and the CERES Surface Validation Group for logistical support at COVE, Theodore Bugtong for logistical support at the Wallops Facilities, the University of Washington CV-580 aircraft crew, Brent Holben and the NASA Aerosol Robotic Network, Dr. Artemio Plana Fattori for all experimental contribution, the EOS Project Office, and the MODIS Science Team. We thank also Reto Stockli for the production of the original averaged MODIS level 3 images. We thank both reviewers for very valuable comments and contributions and FAPESP for their financial support.

REFERENCES

- Artaxo, P., and C. Orsini, 1987: PIXE and receptor models applied to remote aerosol source apportionment in Brazil. *Nucl. Instrum. Methods Phys. Res.*, **B22**, 259–263.
- Campbell, J. L., 1995: Instrumentation, fundamentals, and quantification. *Particle Induced X-Ray Emission Spectrometry*, S. E. Johansson, J. L. Campbell, and K. G. Malmqvist, Eds., John Wiley & Sons, 19–99.
- Castanho, A. D. A., and P. Artaxo, 2001: São Paulo aerosol source apportionment for wintertime and summertime. *Atmos. Environ.*, **35**, 4889–4902.
- Colarco, P., and Coauthors, 2003: Saharan dust transport to the Caribbean during PRIDE: 2. Transport, vertical profiles, and deposition in simulations of in situ and remote sensing observations. *J. Geophys. Res.*, **108**, 8590, doi:10.1029/2002JD002659.
- Hegg, D. A., J. Livingston, P. V. Hobbs, T. Novakov, and P. Russell, 1997: Chemical apportionment of aerosol column optical depth off the mid-Atlantic coast of the United States. *J. Geophys. Res.*, **102** (D21), 25 293–25 303.
- Holben, B. N., and Coauthors, 1998: AERONET—A federated instrument network and data archive for aerosol characterization. *Remote Sens. Environ.*, **66**, 1–16.
- Hopke, P. K., 1991: *Receptor Modeling for Air Quality Management*. Elsevier, 329 pp.
- , Y. Xie, T. Raunema, S. Biegalski, S. Landsberger, W. Maenhaut, P. Artaxo, and D. Cohen, 1997: Characterization of the Gent stacked filter unit PM_{10} sampler. *Aerosol Sci. Technol.*, **27**, 726–735.

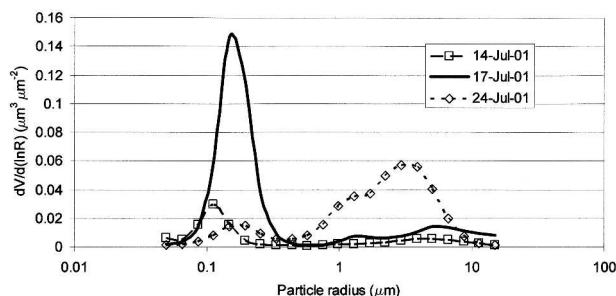


FIG. 8. Particle volume size distribution derived from AERONET sun photometer measurements located at Wallops Island. The size distributions show three aerosol regimes: the regular background with pollution and sea salt (14 Jul, \square), a strong regional pollution (17 Jul, —), and long-range transported dust (24 Jul, \diamond).

- Kalnay, E., M. Kanamitsu, and W. E. Baker, 1990: Global numerical weather prediction at the National Meteorological Center. *Bull. Amer. Meteor. Soc.*, **71**, 1410–1428.
- Kaufman, Y. J., D. Tanré, L. A. Remer, E. F. Vermote, A. Chu, and B. N. Holben, 1997: Operational remote sensing of tropospheric aerosol over land from EOS Moderate Resolution Imaging Spectroradiometer. *J. Geophys. Res.*, **102** (D14), 17 051–17 067.
- Levy, R. C., and Coauthors, 2003: Evaluation of the Moderate-Resolution Imaging Spectroradiometer (MODIS) retrievals of dust aerosol over the ocean during PRIDE. *J. Geophys. Res.*, **108**, 8594, doi:10.1029/2002JD002460.
- Magi, B. I., and P. V. Hobbs, 2003: Effects of humidity on aerosols in southern Africa during the biomass burning season. *J. Geophys. Res.*, **108**, 8495, doi:10.1029/2002JD002144.
- , —, T. W. Kirchstetter, T. Novakov, D. A. Hegg, S. Gao, J. Redemann, and B. Schmid, 2005: Aerosol properties and chemical apportionment of aerosol optical depth at locations off the United States East Coast in July and August 2001. *J. Atmos. Sci.*, **62**, 919–933.
- Novakov, T., D. A. Hegg, and P. V. Hobbs, 1997: Airborne measurements of carbonaceous aerosols on the East Coast of the United States. *J. Geophys. Res.*, **102** (D25), 30 023–30 030.
- Prospero, J. M., R. A. Glaccum, and R. T. Nees, 1981: Atmospheric transport of soil dust from Africa to South America. *Nature*, **289**, 570–572.
- Reid, J. S., P. V. Hobbs, C. Lioussé, J. V. Martins, R. E. Weiss, and T. F. Eck, 1998: Comparison of techniques for measuring short-wave absorption and black carbon content of aerosol from biomass burning in Brazil. *J. Geophys. Res.*, **103** (D24), 32 031–32 040.
- , and Coauthors, 2003: Analysis of measurements of Saharan dust by airborne and groundbased remote sensing methods during the Puerto Rico Dust Experiment (PRIDE). *J. Geophys. Res.*, **108**, 8586, doi:10.1029/2002JD002493.
- Schoeberl, M. R., and L. C. Sparling, 1995: Trajectory modeling. *Diagnostics Tools in Atmospheric Physics*, Vol. 124, G. Fiocco and G. Visconti, Eds., North-Holland, 289–305.
- Smith, W. L., Jr., and Coauthors, 2001: The Chesapeake Lighthouse and Aircraft Measurements for Satellites (CLAMS) experiment. Preprints, *11th Satellite Meteorology and Oceanography Conf.*, Madison, WI, Amer. Meteor. Soc., 492–495.
- Sweet, C. W., and D. F. Gatz, 1998: Short communication summary and analysis of available PM_{2.5} measurements in Illinois. *Atmos. Environ.*, **32**, 1129–1133.
- Tabacniks, M., C. Orsini, and P. Artaxo, 1987: PIXE analysis for air pollution source apportionment in urban areas of Brazil. *Nucl. Instrum. Methods Phys. Res.*, **B22**, 315–318.
- Tanré, D., Y. J. Kaufman, M. Herman, and S. Mattoo, 1997: Remote sensing of aerosol properties over oceans using the MODIS/EOS spectral radiances. *J. Geophys. Res.*, **102**, 16 971–16 988.
- Thurston, G. D., and J. D. Spengler, 1985: A quantitative assessment of source contributions to inhalable particle mass pollution in metropolitan Boston. *Atmos. Environ.*, **19**, 9–25.
- Weiss, R. E., T. V. Larson, and A. P. Waggoner, 1982: In situ rapid response measurements of H₂SO₄/(NH₄)₂SO₄ aerosols in rural Virginia. *Environ. Sci. Technol.*, **16**, 525–532.